Geometric orbital susceptibility: Quantum metric without Berry curvature

Frédéric Piéchon,[1,*] Arnaud Raoux,[1,2] Jean-Noël Fuchs,[1,3] and Gilles Montambaux[1]

[1]*Laboratoire de Physique des Solides, CNRS, Univ. Paris-Sud, Université Paris-Saclay, 91405 Orsay Cedex, France*

[2]*Département de Physique, École Normale Supérieure, PSL Research University, 24 rue Lhomond, 75005 Paris, France*

[3]*Laboratoire de Physique Théorique de la Matière Condensée, CNRS, Université Pierre et Marie Curie,*
4, place Jussieu, 75252 Paris Cedex 05, France

The orbital magnetic susceptibility of an electron gas in a periodic potential depends not only on the zero field energy spectrum but also on the geometric structure of cell-periodic Bloch states which encodes interband effects. In addition to the Berry curvature, we explicitly relate the orbital susceptibility of two-band models to a *quantum metric tensor* defining a distance in Hilbert space. Within a simple tight-binding model allowing for a tunable Bloch geometry, we show that interband effects are essential *even in the absence of Berry curvature*. We also show that for a flat band model, the quantum metric gives rise to a very strong orbital paramagnetism.

I. INTRODUCTION

The orbital susceptibility [1] measures the response of a time reversal invariant electronic system to an external magnetic field B and is defined as the second derivative of the grand potential. Although being a thermodynamic quantity obtained in a perturbative limit ($B \to 0$), its evaluation is not simple, since it has been known for a long time that it depends not only on the zero-field band energy spectrum [2,3] but also on the wave functions which encode interband effects [4–11].

One well-known quantity which describes interband effects is the Berry curvature [12]. For example, it enters—together with the orbital magnetic moment—in the expression of the magnetization, the first derivative of the grand potential with respect to the magnetic field [13–15]. It also appears in the expression of the susceptibility, but other geometrical quantities are expected since the susceptibility is a second derivative with respect to the magnetic field [7,16]. Here we explicitly relate the susceptibility to the *quantum geometric tensor* introduced by M.V. Berry, whose imaginary part is the Berry curvature and whose real part is the so-called *quantum metric tensor* [17,18]. The main goal of this paper is to show the central role played by this metric tensor on the structure of the orbital susceptibility.

Until recently the metric tensor was considered as a theoretical object useful to characterize the localization properties of Wannier functions in band insulators [19,20]. However few recent works have suggested different physical properties such as current noise and superfluid weight that depend on the quantum metric in an essential way [21–23]. Moreover, in artificial crystals made of cold atoms, a full reciprocal space map of the quantum metric should be accessible via Stückelberg interferometry [24].

In a recent paper, we derived a general formula for the orbital susceptibility within a tight-binding picture (restricted here to $d = 2$ dimensions) [25]:

$$\chi_{\mathrm{orb}}(\mu, T) = -\frac{\mu_0 e^2}{12\hbar^2} \frac{\Im m}{\pi S} \int_{-\infty}^{\infty} n_{\mathrm{F}}(E) \mathrm{Tr}\, \hat{X} \, dE \,, \quad (1)$$

where the operator $\hat{X}$ is written in terms of the zero-field Green function $\hat{g}$ and of the derivatives ∂_x and ∂_y of the Bloch Hamiltonian $\hat{h}(\boldsymbol{k})$ with respect to the components k_x and k_y of the wave vector:

$$\hat{X} = \hat{g}\, \partial_x^2 \hat{h}\, \hat{g}\, \partial_y^2 \hat{h} - \hat{g}\, \partial_{xy}^2 \hat{h}\, \hat{g}\, \partial_{xy}^2 \hat{h} + 2([\hat{g}\, \partial_x \hat{h}, \hat{g}\, \partial_y \hat{h}])^2 \,. \quad (2)$$

Moreover, the orbital susceptibility was shown to satisfy a general sum rule over the full bandwidth [26–28]:

$$\int \chi_{\mathrm{orb}}(\mu, T)\, d\mu = 0 \,. \quad (3)$$

Although Eq. (1) is complete (checked against numerical calculations for various models [25]), it hides many subtle effects that we wish to discuss here in the simplest context of two-band models.

The outline of this paper is as follows: Section II presents the quantum geometric properties that characterize the cell-periodic Bloch states $|u_\alpha(\boldsymbol{k})\rangle$ of a given energy band $\epsilon_\alpha(\boldsymbol{k})$. In particular, in addition to the well-known Berry curvature tensor $\Omega_{\alpha ij}$ we also introduce the quantum metric tensor $g_{\alpha ij}$ as a measure of the distance between Bloch states. Section III presents a general formula for the orbital susceptibility χ_{orb} of two-band models. It is shown that, in contrast to the intraband Landau-Peierls contributions χ_{LP} which depends only on the energy band spectrum, the interband contribution χ_{inter} crucially depends on the quantum geometry of Bloch states. More precisely χ_{inter} may be decomposed in three contributions $\chi_{\mathrm{inter}} = \chi_\Omega + \chi_g + \tilde{\chi}_g$ where χ_Ω depends only on the Berry curvature whereas χ_g and $\tilde{\chi}_g$ depend only on the quantum metric. Details of the derivation are given in Appendix A. In Sec. IV we present explicit calculations of the different orbital susceptibility contributions for particular models that were designed in order to highlight the physics hidden in the three interband geometric contributions. Section V provides a more heuristic derivation and also suggests a possible qualitative interpretation for each of the three interband geometric contributions. In particular χ_Ω is interpreted as a measure of the $\boldsymbol{k}$-space fluctuations of the spontaneous orbital magnetization whereas χ_g and $\tilde{\chi}_g$ are interpreted as field induced effects resulting from the field induced horizontal and vertical positional shifts [29]. Appendix B provides more

*piechon@lps.u-psud.fr

details on these positional shifts. In Sec. VI we explain how our formulation compares with previous works; more precisely we discuss Blount's formula [7] and also the more recent susceptibility formula obtained by Gao *et al.* [16]. The paper ends with a conclusion and perspectives.

II. GEOMETRY: QUANTUM METRIC AND BERRY CURVATURE

In order to describe the evolution of a cell-periodic Bloch state $|u_\alpha(\boldsymbol{k})\rangle$ under the variation of a vector parameter $\boldsymbol{k}$, M.V. Berry introduced the *quantum geometric tensor* T_α:

$$T_{\alpha ij}(\boldsymbol{k}) = \langle \partial_i u_\alpha | 1 - \mathscr{P}_\alpha | \partial_j u_\alpha \rangle , \qquad (4)$$

where $\mathscr{P}_\alpha(\boldsymbol{k}) = |u_\alpha\rangle\langle u_\alpha|$ is the projector on the band α of energy $\varepsilon_\alpha(\boldsymbol{k})$. The imaginary (antisymmetric) part of $T_{\alpha ij}$ is nothing but the Berry curvature tensor: $\Omega_{\alpha ij}(\boldsymbol{k}) = -2 \operatorname{Im} T_{\alpha ij}$. The real (symmetric) part, named the *quantum metric tensor* $g_{\alpha ij}$, characterizes a distance in Hilbert space, defined as [18]:

$$ds_\alpha^2 \equiv 1 - |\langle u_\alpha(\boldsymbol{k})|u_\alpha(\boldsymbol{k} + d\boldsymbol{k})\rangle|^2 . \qquad (5)$$

Expanding the $\boldsymbol{k}$ dependence of the wave functions to second order, the tensor $g_{\alpha ij}$ is defined as

$$ds_\alpha^2 = g_{\alpha ij} \, dk^i \, dk^j \quad \text{with} \quad g_{\alpha ij}(\boldsymbol{k}) = \operatorname{Re} T_{\alpha ij} . \qquad (6)$$

The curvature and quantum metric tensors have the $\boldsymbol{k}$-space periodicity of the *reciprocal lattice* even if the Bloch states $|u_\alpha\rangle$ do not have it. Moreover, they stay invariant upon a *Berry gauge* transformation $|u_\alpha\rangle \to e^{i\varphi_\alpha(\boldsymbol{k})}|u_\alpha\rangle$. Systems with time reversal symmetry verify $\Omega_{\alpha ij}(-\boldsymbol{k}) = -\Omega_{\alpha ij}(\boldsymbol{k})$ and $g_{\alpha ij}(-\boldsymbol{k}) = g_{\alpha ij}(\boldsymbol{k})$. Centrosymmetric systems verify $\Omega_{\alpha ij}(-\boldsymbol{k}) = \Omega_{\alpha ij}(\boldsymbol{k})$. In the following, to simplify further notations, the $\boldsymbol{k}$ dependence of quantities will be explicitly written only in their definitions.

We now restrict to two-band models. The $\boldsymbol{k}$-space Hamiltonian matrix can be written as

$$\hat{h}(\boldsymbol{k}) = \varepsilon_0(\boldsymbol{k})\mathbb{1} + \boldsymbol{h}(\boldsymbol{k}) \cdot \boldsymbol{\sigma} = \varepsilon_0(\boldsymbol{k})\mathbb{1} + \varepsilon(\boldsymbol{k})\boldsymbol{n}(\boldsymbol{k}) \cdot \boldsymbol{\sigma}, \qquad (7)$$

where $\boldsymbol{\sigma}$ is the vector of Pauli matrices, and $\boldsymbol{n}(\boldsymbol{k})$ is a three-dimensional unit vector depending on the d-dimensional vector $\boldsymbol{k}$. The Hamiltonian matrix has two eigenvalues $\varepsilon_\alpha(\boldsymbol{k}) = \varepsilon_0(\boldsymbol{k}) + \alpha\varepsilon(\boldsymbol{k})$ with corresponding projectors $\mathscr{P}_\alpha(\boldsymbol{k}) = \frac{1}{2}(\mathbb{1} + \alpha\boldsymbol{n} \cdot \boldsymbol{\sigma})$ where $\alpha = \pm$. In that situation, the Berry curvature and metric tensor components verify $\Omega_{\alpha ij} \equiv \alpha\Omega_{ij}$ and $g_{\alpha ij} \equiv g_{ij}$ with

$$\Omega_{ij}(\boldsymbol{k}) = \frac{1}{2}(\partial_i \boldsymbol{n} \times \partial_j \boldsymbol{n}) \cdot \boldsymbol{n} , \quad g_{ij}(\boldsymbol{k}) = \frac{1}{4}\partial_i \boldsymbol{n} \cdot \partial_j \boldsymbol{n}, \qquad (8)$$

where each component of the curvature tensor verifies the identity

$$\Omega_{ij}^2 = 4(g_{ii}g_{jj} - g_{ij}^2). \qquad (9)$$

In other words, for each vector $\boldsymbol{k}$, the quantum metric determines the modulus of the Berry curvature but not its $\boldsymbol{k}$ dependent sign. In this paper we consider more specifically the case of $d = 2$. In that situation the Berry curvature tensor has a single nonvanishing component $\Omega = \Omega_{xy}$, and the quantum metric tensor g is a 2×2 symmetric matrix with the three elements g_{xx}, g_{yy}, g_{xy}. In addition to the covariant metric tensor $g_{ij}(\boldsymbol{k})$, it is convenient to further introduce a contravariant

metric tensor g^{ij} through the identity $g^{ik}g_{kj} = \det(g)\delta_j^i$ such that

$$(g^{xx}, g^{yy}, g^{xy}) \equiv (g_{yy}, g_{xx}, -g_{xy}). \qquad (10)$$

The identity (9) can then be rewritten as

$$\Omega^2 = 4\det g = 4g_{ij}g^{ij}. \qquad (11)$$

The quantum geometric tensor of each band can then be written as

$$T_\alpha(\boldsymbol{k}) = \frac{\operatorname{Tr} g}{2}(\mathbb{1} + \boldsymbol{\tau}_\alpha \cdot \boldsymbol{\sigma}) \qquad (12)$$

with the unit vector

$$\boldsymbol{\tau}_\alpha(\boldsymbol{k}) \equiv \frac{1}{\operatorname{Tr} g}(2g_{xy}, \alpha\Omega, g_{xx} - g_{yy}). \qquad (13)$$

For systems with time reversal symmetry the vector $\boldsymbol{\tau}_\alpha(\boldsymbol{k})$ has the same symmetry properties as $\boldsymbol{n}(\boldsymbol{k})$. Note that in artificial crystals made of cold atoms, a full reciprocal space map of the quantum metric tensor $T_\alpha(\boldsymbol{k})$ should be accessible via Stückelberg interferometry [24].

III. ORBITAL SUSCEPTIBILITY FOR TWO-BAND MODELS

We now analyze the different contributions to the orbital susceptibility; the details of their explicit derivation are given in Appendix A. Quite generally, the orbital susceptibility can be decomposed in

$$\chi_{\text{orb}} = \chi_{\text{LP}} + \chi_{\text{inter}}, \qquad (14)$$

where the first term called Landau-Peierls (LP) only involves the zero field band spectrum whereas the second term, here referred to as interband, encodes all wave functions' geometric effects.

A. Landau-Peierls contribution

The Landau-Peierls (LP) contribution χ_{LP} writes (in units of $\frac{\mu_0 e^2}{\hbar^2}$) [3]:

$$\chi_{\text{LP}}(\mu, T) = \left\langle \frac{n_\alpha'}{12}\left(\partial_x^2\varepsilon_\alpha \, \partial_y^2\varepsilon_\alpha - \partial_{xy}^2\varepsilon_\alpha \, \partial_{xy}^2\varepsilon_\alpha\right)\right\rangle_{\text{BZ}} \qquad (15)$$

with the shorthand notations used throughout the paper

$$n_\alpha \equiv n_F(\varepsilon_\alpha(\boldsymbol{k})), \quad \langle \bullet \rangle_{\text{BZ}} \equiv \sum_{\alpha=\pm} \int \bullet \frac{d^2k}{4\pi^2} \qquad (16)$$

and where $n_F(\varepsilon)$ is the Fermi factor. This LP contribution only involves the energy spectrum and its Hessian near the Fermi level. At parabolic band edges, it reduces to Landau diamagnetism with the effective band mass. By contrast, in the vicinity of a Van Hove singularity it is strongly paramagnetic because the spectrum exhibits a saddle point and therefore masses of opposite sign [30]. In the multiband case, χ_{LP} verifies the sum rule (3) for each band separately. Being a Fermi level property [see the n_α' factor in Eq. (15)], *the LP contribution vanishes in a gap.*

B. Interband geometric contributions

We now come to the structure of the interband contribution χ_{inter}. It may itself be decomposed in three contributions as

$$\chi_{\text{inter}} = \chi_\Omega + \chi_g + \tilde{\chi}_g, \tag{17}$$

which explicitly depend on either the Berry curvature or the metric tensor, and which separately obey the sum rule (3):

$$\int d\mu \chi_\Omega(\mu) = \int d\mu \chi_g(\mu)$$
$$= \int d\mu \tilde{\chi}_g(\mu) = 0. \tag{18}$$

The first contribution χ_Ω is written in terms of the Berry curvature Ω:

$$\chi_\Omega = \left\langle \left(-n'_\alpha + \alpha \frac{n_\alpha}{\varepsilon} \right) \mathscr{M}^2 \right\rangle_{\text{BZ}}, \quad \mathscr{M} = \varepsilon \Omega . \tag{19}$$

The term proportional to n'_α can be understood as the Pauli paramagnetic contribution of the orbital magnetic moment $\mathscr{M}(\boldsymbol{k}) = \varepsilon \Omega$ [7,16,31]. Being a Fermi surface term, it vanishes in a band gap. The term proportional to n_α is always diamagnetic. Moreover, being a Fermi sea term it gives rise to a *plateau* in a band gap. Due to the absence of Berry curvature, χ_Ω vanishes in centrosymmetric systems.

The contribution χ_g may be seen as more fundamental since it is related to the metric tensor, which never vanishes for coupled bands. It may be compactly written as a pure Fermi sea term:

$$\chi_g = \left\langle \left(-\alpha \frac{n_\alpha}{\varepsilon} \right) Z_g \right\rangle_{\text{BZ}}, \quad Z_g = \frac{1}{2} \partial_j (\varepsilon^2 \, \partial_i g^{ij}), \tag{20}$$

where Z_g explicitly involves the contravariant metric tensor g^{ij} that was defined in (10). This quantity $Z_g(\boldsymbol{k})$ changes sign in the BZ and verifies $\int d^2k \, Z_g(\boldsymbol{k}) = 0$. As a consequence, $\chi_g(\mu)$ may exhibit a diamagnetic or paramagnetic *plateau* in a band gap.

The third contribution $\tilde{\chi}_g$ only appears in the absence of particle-hole symmetry. It may also be written as pure Fermi sea contribution that depends on the metric tensor:

$$\tilde{\chi}_g = \left\langle \left(-\alpha \frac{n_\alpha}{\varepsilon} \right) \tilde{Z}_g \right\rangle_{\text{BZ}} \tag{21}$$

$$\tilde{Z}_g = g^{ij} \, \partial_i \varepsilon_0 \, \partial_j \varepsilon_0 + \alpha \varepsilon \, \partial_i (g^{ij} \, \partial_j \varepsilon_0). \tag{22}$$

The first term of $\tilde{Z}_g(\boldsymbol{k})$ is always positive and thus leads to a paramagnetic plateau in a gap. The second part changes its sign with band index α, and its BZ average vanishes in a gap.

IV. EXAMPLES

This section presents explicit calculations of the different contributions to the orbital susceptibility. We discuss particular models that were designed in order to highlight the physics hidden in the three interband geometric contributions and also to illustrate their quantitative importance. We first consider a lattice model with particle-hole symmetry (such that $\tilde{\chi}_g = 0$) for which the relative importance of the interband contributions χ_Ω and χ_g can be tuned by a continuous parameter. We show in particular the importance of the geometric tensor, *even in the absence of Berry curvature*. In a second example

we discuss the important differences between a lattice model and its low energy counterpart. This remark underlines the approximations done when the spectrum is linearized near the edges of a band gap. The last example concerns a lattice model that is inversion symmetric (such that $\chi_\Omega = 0$) but extremely particle-hole asymmetric since it exhibits a flat band. This flat band gives rise to a huge contribution $\tilde{\chi}_g$. For comparison purposes, we also present calculations of the corresponding spin contribution which, in the absence of spin-orbit coupling, is limited to the Pauli susceptibility χ_{spin} which is simply proportional to the zero-field density of states.

A. From square to honeycomblike lattice

We consider a toy-model of electrons hopping on a tunable brick-wall lattice with a staggered on-site potential Δ. The tunable hopping parameter λ interpolates between a square lattice ($\lambda = 1$) where the Berry curvature is zero and a distorted honeycomb lattice ($\lambda = 0$) where there is a finite Berry curvature concentrated in the vicinity of the Dirac points. The model is illustrated in Fig. 1(a). Setting the nearest-neighbor coupling $t = 1$ and the interatomic distance $a = 1$, the corresponding Hamiltonian [cf. Eq. (7)] is given by the vector $\boldsymbol{h}(\boldsymbol{k}) = [2\cos k_x + (1 + \lambda)\cos k_y, (1 - \lambda)\sin k_y, \Delta]$.

First, consider the case of the square lattice ($\lambda = 1$). The energy spectrum has two bands separated by a gap 2Δ. The density of states [proportional to the Pauli spin susceptibility χ_{spin} plotted in Fig. 1(f)] exhibits Van Hove singularities at gap edges. The orbital susceptibility $\chi_{\text{orb}}(\mu) = \chi_{\text{LP}} + \chi_\Omega + \chi_g$ is plotted on the top row of Fig. 1(f). In addition to the Landau diamagnetic behavior at the parabolic band edges, $\chi_{\text{orb}}(\mu)$ exhibits a truncated logarithmic behavior at the gap edges and a paramagnetic plateau in the gap. The Landau-Peierls contribution χ_{LP} properly exhibits Landau diamagnetism at the band edges and also paramagnetic peaks reminiscent of the logarithmic divergence of the density of states at the gap edges. However it vanishes in the gap: Therefore it cannot explain the paramagnetic plateau of χ_{orb} in the gap. For centrosymmetric systems there is no Berry curvature and therefore $\chi_\Omega = 0$. Thus, one naively expects the bands to be uncoupled. However, the quantum metric and Z_g do not vanish but give rise to a contribution χ_g that provides exactly the paramagnetic plateau in the gap. As the gap goes to 0, this plateau diverges as $\log \Delta$. In addition, in order to respect the sum rule, χ_g presents also diamagnetic peaks near the gap edges. This striking example shows that *the interband coupling is not only encoded in the Berry curvature*, and that the metric contribution χ_g is essential to explain the structure of the total susceptibility.

We now consider the limit $\lambda = 0$ defining the brick-wall lattice. It has the same properties as the honeycomb lattice, except that the two Dirac points do not lie on symmetry lines of the BZ. It has been recently used in a cold-atom experiment to probe the existence, the motion, and the merging of these Dirac points under proper variations of hopping parameters [32,33]. For this system, χ_{orb} and its different contributions are presented on the bottom row of Fig. 1(f). In addition to the diamagnetic Landau regime at the band edges and the paramagnetic divergence at the Van Hove singularity, it exhibits a deep diamagnetic plateau in the gap, whose amplitude scales as $1/\Delta$, reminiscent of the diamagnetic δ
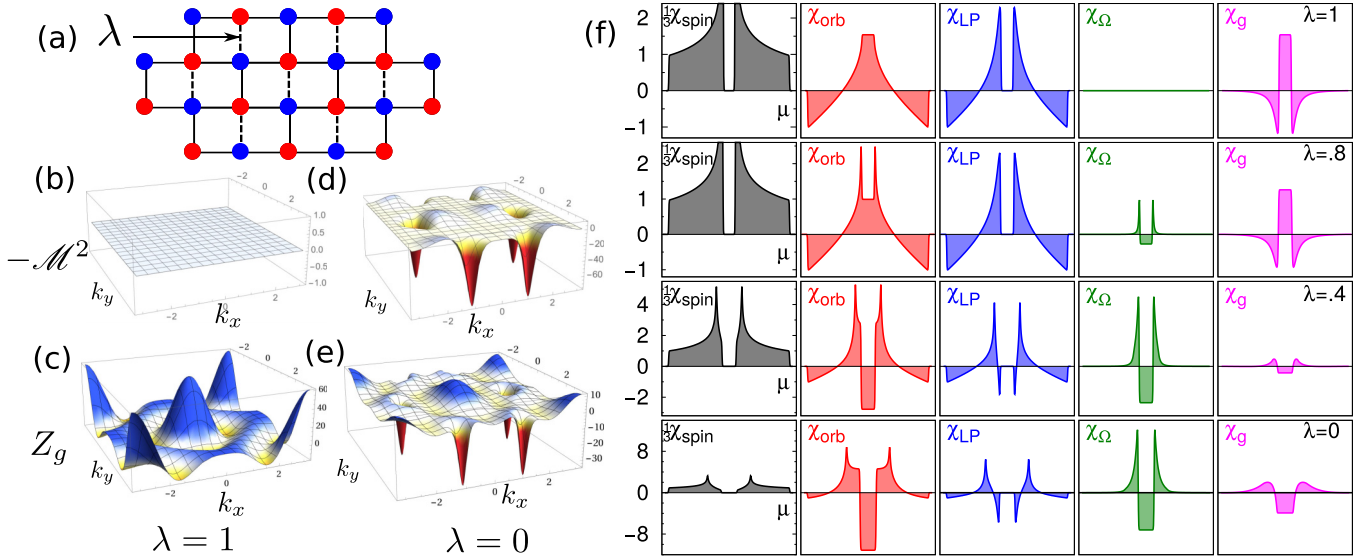
FIG. 1. (a) Tunable brick-wall lattice with a staggered on-site potential Δ: It interpolates between a square ($\lambda = 1$) and a deformed honeycomb (brick wall) ($\lambda = 0$). (b),(d) Berry curvature term $-\mathcal{M}(\mathbf{k})^2$, respectively, for $\lambda = 1$ and 0. (c),(e) Metric term $Z_g(\mathbf{k})$, respectively, for $\lambda = 1$ and 0. For clarity, the area of the plot covers twice the first Brillouin zone. Blue and red colors denote, respectively, positive and negative values. (f) Evolution of the magnetic susceptibility versus chemical potential μ as a function of λ. The first column is the Pauli spin susceptibility which is proportional to the zero field density of states. It is normalized such that $\chi_{\text{spin}} = -3\chi_{\text{orb}}$ at the band edges, as in the absence of a lattice. The four next columns concern the orbital response, respectively, the susceptibility χ_{orb} (red), χ_{LP} (blue), χ_Ω (green), and χ_g (magenta). They are normalized to the Landau susceptibility χ_L at the band edges, which itself depends on λ: $\chi_L(\lambda) = \chi_L(1)\sqrt{\frac{1+3\lambda}{3+\lambda}}$. The half bandwidth, equal to $\sqrt{\Delta^2 + 3 + \lambda}$, is also normalized to unity. We fix $\Delta/t = 0.4$ and $T = 0.001t$.

peak found by McClure in the limit $\Delta \to 0$ [31,34]. As it is well known for the honeycomb lattice, there is a finite Berry curvature concentrated near the two Dirac points, with opposite signs in the two valleys [35], leading to $-\mathcal{M}^2$ plotted in Fig. 1(d). In this situation, the quantity $Z_g(\mathbf{k})$ in Fig. 1(e) shows also large negative peaks near the Dirac points, leading to a diamagnetic χ_g in the gap. Therefore the diamagnetic plateau is due both to the Berry curvature and the quantum metric contributions. Also remarkable is the paramagnetic *plateau* near the edges of the gap [25,26]. This *plateau* arises from the subtle compensation of a diverging diamagnetic peak of χ_{LP}, a diverging paramagnetic peak of χ_Ω, and a smooth paramagnetic contribution χ_g.

Figure 1(f) presents the evolution of the susceptibility and its different contributions [which all obey separately the sum rule (3)] when varying λ from 1 to 0. The contribution related to the Berry curvature, which is zero when inversion symmetry is preserved, monotonously decreases in the gap and increases outside. The geometric contribution χ_g is more involved: Inside the gap it evolves from a paramagnetic to a diamagnetic plateau whereas it has the reverse tendency outside the gap such as to respect the sum rule.

B. Lattice model versus low energy model

This section provides a quantitative comparison of the different susceptibility contributions between the brick-wall lattice model at $\lambda = 0$ and the corresponding linearized low energy effective model in the vicinity of the gapped Dirac points. It is interesting since it emphasizes the approximations which are made when linearizing the graphene electronic

spectrum (similar to the brick-wall lattice) in the vicinity of the gapped Dirac points.

The lattice model at $\lambda = 0$ is given by $h(\mathbf{k}) = [2\cos k_x + \cos k_y, \sin k_y, \Delta]$. The gapped Dirac points are located at $(k_x, k_y) = (\xi \frac{2\pi}{3}, 0)$ with valley index $\xi = \pm 1$. The linearized model describing the vicinity of a Dirac point is given by $h_\xi(\mathbf{k}) = [\xi v_x k_x, v_y k_y, \Delta]$ with $(v_x, v_y) = (\sqrt{3}, 1)$.

For this linearized model it is then straightforward to obtain the equalities

$$3\mathcal{H} = \mathcal{M}^2 = Z_g = \frac{\Delta^2 v_x^2 v_y^2}{4\varepsilon^4}, \qquad (23)$$

where $\mathcal{H}(\mathbf{k}) = \frac{1}{12}[\partial_{xx}^2 \varepsilon \partial_{yy}^2 \varepsilon - (\partial_{xy}^2 \varepsilon)^2]$ and $\varepsilon(\mathbf{k}) = \sqrt{(v_x k_x)^2 + (v_y k_y)^2 + \Delta^2}$. From these equalities, it is also immediate to deduce the explicit analytical form of the different susceptibility contributions in each valley. This is summarized in the following table ($\chi_0 = \frac{1}{8\pi} \frac{v_x v_y}{\Delta}$):

The expression for χ_{orb} corresponds to a diamagnetic plateau in the gap and zero outside the gap. This coincides

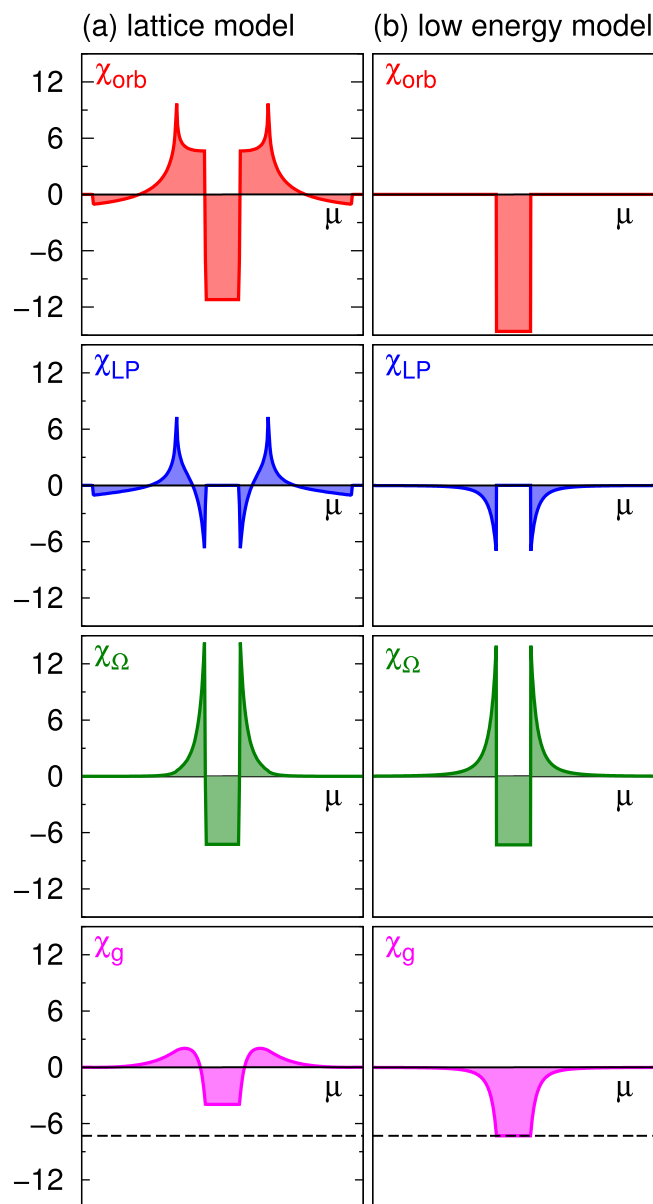|	$|\mu| < \Delta$	$|\mu| > \Delta$
χ_{LP}	0	$-\frac{1}{3}\chi_0 \frac{\Delta^3}{\mu^3}$
χ_Ω	$-\frac{1}{3}\chi_0$	$+\frac{2}{3}\chi_0 \frac{\Delta^3}{\mu^3}$
χ_g	$-\frac{1}{3}\chi_0$	$-\frac{1}{3}\chi_0 \frac{\Delta^3}{\mu^3}$
χ_{orb}	$-\frac{2}{3}\chi_0$	0

FIG. 2. (a) The susceptibility contributions χ_{orb}, χ_{LP}, χ_{Ω}, and χ_g as a function of the chemical potential μ for the lattice model [this is identical to Fig. 1(f) with $\lambda = 0$]. (b) Similar quantities but for the low energy (linearized) model.

exactly with what has been derived directly from the Landau levels of a gapped Dirac spectrum [31]. The present perturbative approach, however, provides the supplementary information that the apparent vanishing of χ_{orb} outside the gap results from the fortuitous compensation of the three contributions $\chi_{\mathrm{LP}}, \chi_{\Omega}$, and χ_g, since each of them is a power-law decreasing function outside the gap.

The quantitative comparison of the expressions for the low energy model with the exact lattice calculations are shown in Fig. 2. One striking feature is that, for the contribution χ_{Ω}, the lattice model and the low energy model calculations almost coincide. In fact, the contribution χ_{Ω} of the linearized model verifies the sum rule. By contrast, for the contribution χ_g there is a large quantitative difference for the value of

the diamagnetic plateau between the lattice model and the low energy model. This difference explains quantitatively the value of the paramagnetic plateau (at gap edges) of χ_{orb} for the lattice model. To summarize, we have shown that if χ_{Ω} essentially depends on the vicinity of the Dirac points, accounting quantitatively for χ_g requires us to consider the whole Brillouin zone.

C. Mielke's checkerboard lattice model

As an illustration of a non-particle-hole symmetric system, we consider a toy model exhibiting a flat band. This is the Mielke checkerboard lattice shown in Fig. 3(a), where all hopping integrals are identical ($t = \frac{1}{2}$) [36,37]. The corresponding Hamiltonian is characterized by the vector $\boldsymbol{h}(\boldsymbol{k}) = (\cos k_x + \cos k_y, 0, \sin k_x \sin k_y)$ and the energy $\varepsilon_0(\boldsymbol{k}) = \varepsilon(\boldsymbol{k}) - 1$ [see Eq. (7)]. The spectrum, shown in Fig. 3(b), consists of a flat band touching the bottom of a dispersion relation which is that of the square lattice. One could expect naively the flat band to be inert in a magnetic field and the susceptibility to be simply given by the LP response of the square lattice [blue curve in Fig. 3(c)]. The exact result (red curve) is dramatically different, showing the importance of interband effects in this case. Because of inversion symmetry, there is no Berry curvature and $\chi_{\Omega} = 0$, and therefore only the metric dependent terms χ_g and $\tilde{\chi}_g$ can account for the strong interband effects. The most striking feature is the diverging paramagnetic peak of χ_{orb} when approaching the energy of the flat band. Away from the flat band, this peak appears partially compensated by a wide diamagnetic shoulder. These two features come, respectively, from the first and second term in $\tilde{\chi}_g$. In fact, the contribution χ_g appears completely shadowed by that of $\tilde{\chi}_g$. Both contributions show, however, that interband effects extend far away in energy
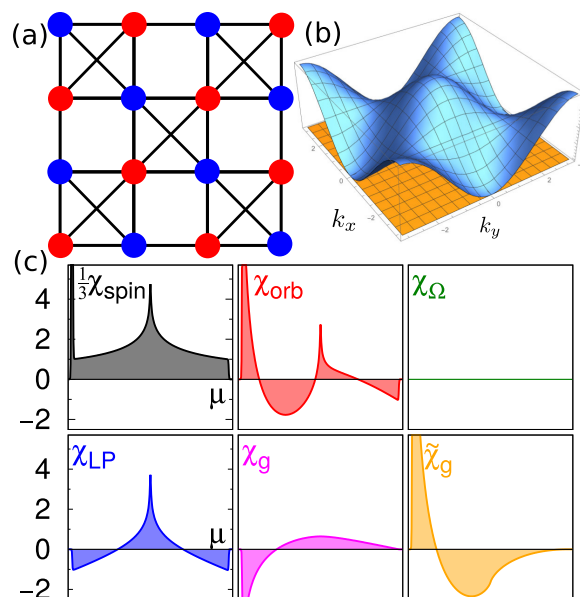

FIG. 3. Top: (a) The checkerboard lattice (here there is no on-site potential) and (b) the corresponding energy spectrum. Bottom: (c) Pauli spin susceptibility and orbital susceptibility χ_{orb} with its different contributions as a function of the chemical potential. Units for χ and μ are similar to Fig. 1(f).

from the flat band. As a last remark, we note that Tasaki's two-band model on the square lattice [37,38], which exhibits a flat band separated by a finite gap from the dispersive band, gives rise to vanishing contributions $\tilde{\chi}_g$ and χ_Ω and a finite contribution χ_g with a paramagnetic plateau in the gap.

V. HEURISTIC DERIVATION AND INTERPRETATION OF INTERBAND GEOMETRIC CONTRIBUTIONS

This section presents a heuristic derivation and an interpretation of the three interband susceptibility contributions $\chi_\Omega, \chi_g, \tilde{\chi}_g$. To this end, it appears instructive to recall known results for the spontaneous orbital magnetization.

For generic multiband systems, the spontaneous orbital magnetization is given by [12]

$$M(\mu, T) = \left\langle \left[n_\alpha \mathscr{M}_\alpha + T \ln(1 + e^{-(\varepsilon_\alpha - \mu)/T}) \Omega_\alpha \right] \right\rangle_{\text{BZ}}, \quad (24)$$

where $\mathscr{M}_\alpha(\boldsymbol{k})$ is the orbital magnetic moment and $\Omega_\alpha(\boldsymbol{k})$ is the Berry curvature of the band of energy $\varepsilon_\alpha(\boldsymbol{k})$. For time reversal invariant systems considered here, the spontaneous orbital magnetization vanishes because $\mathscr{M}_\alpha(\boldsymbol{k}) = -\mathscr{M}_\alpha(-\boldsymbol{k})$ and $\Omega_\alpha(\boldsymbol{k}) = -\Omega_\alpha(-\boldsymbol{k})$. For a system that breaks time reversal symmetry, $M(\mu)$ can be nonzero however it has to verify the sum rule $\int d\mu \, M(\mu) = 0$, valid for any multiband tight-binding model. Although formula (24) has been demonstrated in various ways [12,25], a useful heuristic derivation or reinterpretation consists of differentiating the grand canonical potential

$$F(\mu, B, T) = -T \int d\epsilon \, \rho(\epsilon, B) \ln(1 + e^{-(\epsilon - \mu)/T}), \quad (25)$$

to first order in magnetic field, with an effective magnetic field dependent density of states of the form [12]

$$\rho(\epsilon, B) = \langle (1 + B\Omega_\alpha) \delta(\epsilon - \varepsilon_\alpha + \mathscr{M}_\alpha B) \rangle_{\text{BZ}}. \quad (26)$$

The factor $(1 + B\Omega_\alpha)$ is interpreted as a correction to the phase-space integration measure and $-\mathscr{M}_\alpha B$ as a Zeeman-like correction of orbital origin to the band energy at first order in magnetic field. To finish with the spontaneous orbital magnetization, we note that for two-band systems $\mathscr{M}_\alpha = \alpha\varepsilon\Omega_\alpha$ and $\Omega_\alpha = \alpha\Omega$, such that by introducing the two-dimensional Berry connection vector $\boldsymbol{a}_\alpha(\boldsymbol{k}) = i\langle u_\alpha | \nabla_k | u_\alpha \rangle$ and using the identity $\Omega_\alpha = [\nabla_k \times \boldsymbol{a}_\alpha]_z$, the spontaneous magnetization Eq. (24) of two-band systems can be recast in the form

$$M(\mu, T) = \langle n_\alpha (\alpha\varepsilon [\nabla_k \times \boldsymbol{a}_\alpha]_z + [\boldsymbol{v}_\alpha \times \boldsymbol{a}_\alpha]_z) \rangle_{\text{BZ}}, \quad (27)$$

with $\boldsymbol{v}_\alpha(\boldsymbol{k}) = \nabla_k \varepsilon_\alpha$ the band velocity and where the second term in Eq. (27) follows from an integration by part of the second term in Eq. (24).

We now come to the heuristic derivation of the three interband susceptibility contributions. The idea consists of finding the modified effective density of states, valid to second order in magnetic field that permits us to obtain the three contributions $\chi_\Omega, \chi_g, \tilde{\chi}_g$ from the second order derivative of the grand potential. For two band systems we obtain the following effective density of states:

$$\rho(\epsilon, B) = \left\langle (1 + B\Omega_\alpha) \delta \left(\epsilon - \varepsilon_\alpha + \mathscr{M}_\alpha B - \tfrac{1}{2} \mathscr{M}_\alpha \Omega_\alpha B^2 \right) \right\rangle_{\text{BZ}}, \quad (28)$$

where now $\Omega_\alpha(B)$ and $\mathscr{M}_\alpha(B)$ are field dependent quantities given by

$$\Omega_\alpha(B) = [\nabla_k \times \boldsymbol{a}_\alpha]_z + \frac{B}{2}\alpha[\nabla_k \times \tilde{\boldsymbol{a}}_g]_z, \quad (29)$$

$$\mathscr{M}_\alpha(B) = \alpha\varepsilon \left(\Omega_\alpha(B) + \frac{B}{2} \frac{[\nabla_k \times \varepsilon^2 \boldsymbol{a}_g]_z}{\varepsilon^2} \right), \quad (30)$$

where $\boldsymbol{a}_\alpha$ is the zero-field Berry connection and $\boldsymbol{a}_g, \tilde{\boldsymbol{a}}_g$ are the first order field induced corrections [29] that verify (see appendix B for more details)

$$\Omega_g(\boldsymbol{k}) = [\nabla_k \times \boldsymbol{a}_g]_z = -\tfrac{1}{2} \partial_i \partial_j g^{ij}, \quad (31)$$

$$\tilde{\Omega}_g(\boldsymbol{k}) = [\nabla_k \times \tilde{\boldsymbol{a}}_g]_z = -\partial_i \left(\frac{g^{ij} \partial_j \varepsilon_0}{\varepsilon} \right). \quad (32)$$

Within this picture, χ_Ω is given by

$$\chi_\Omega = \left\langle \left(-n'_\alpha \mathscr{M}_\alpha^2 + n_\alpha \mathscr{M}_\alpha \Omega_\alpha \right) \right\rangle_{\text{BZ}}, \quad (33)$$

where $\mathscr{M}_\alpha = \alpha\varepsilon\Omega_\alpha$ and $\Omega_\alpha = \alpha\Omega$ are the zero field orbital magnetic moment and Berry curvature. The contribution χ_Ω is thus a quadratic function of the quantities $\mathscr{M}_\alpha, \Omega_\alpha$ that appear linearly in the orbital magnetization formula Eq. (24). This suggests that a natural interpretation for χ_Ω is a measure of the $\boldsymbol{k}$-space fluctuations of the spontaneous orbital magnetization (the $\boldsymbol{k}$-space average of which vanishes). By contrast, χ_g and $\tilde{\chi}_g$ depend linearly on, respectively, $\boldsymbol{a}_g$ and $\tilde{\boldsymbol{a}}_g$:

$$\chi_g = \left\langle n_\alpha \, \alpha\varepsilon \left(\frac{[\nabla_k \times \varepsilon^2 \boldsymbol{a}_g]_z}{\varepsilon^2} \right) \right\rangle_{\text{BZ}},$$
$$\tilde{\chi}_g = \langle n_\alpha (\alpha\varepsilon [\nabla_k \times \tilde{\boldsymbol{a}}_g]_z + [\boldsymbol{v}_\alpha \times \tilde{\boldsymbol{a}}_g]_z) \rangle_{\text{BZ}}. \quad (34)$$

The form of $\tilde{\chi}_g$ being identical to the equality (27), it strongly suggests to interpret the quantity $\tilde{\chi}_g B$ as an induced magnetization. By extension, we suggest that $\chi_g B$ may be interpreted as a field induced orbital magnetization resulting from a field induced orbital magnetic moment $\alpha\varepsilon \frac{B}{2} \frac{[\nabla_k \times \varepsilon^2 \boldsymbol{a}_g]_z}{\varepsilon^2}$.

VI. COMPARISON WITH OTHER WORKS

Many different approaches were developed to calculate the orbital susceptibility in multiband systems (see discussion in Refs. [25,39]). Compact but abstract orbital susceptibility formulas were obtained using Green's function techniques. Other approaches usually result in an orbital susceptibility that is composed of several contributions. The main object of this section is to discuss the different decompositions that were obtained for the interband contribution $\chi_{\text{inter}}(\mu)$. Before discussing specific works, it is worth mentioning some generic features of the interband contribution $\chi_{\text{inter}}(\mu)$. Quite generally $\chi_{\text{inter}}(\mu)$ may be formally written as the sum of individual band contribution $\chi_{\text{inter},\alpha}(\mu)$ where each $\chi_{\text{inter},\alpha}(\mu)$ is composed of both Fermi surface and Fermi sea contributions. For each band, the Fermi surface term depends on n'_α and thus vanishes outside the energy band. By contrast the Fermi sea term proportional to n_α gives rise to a finite susceptibility plateau for all μ above the top edge of the αth band. As a consequence the integrated contribution $\int d\mu \, \chi_{\text{inter},\alpha}(\mu)$ is infinite. In retrospect, this result

implies that the decomposition of $\chi_{\text{inter}}(\mu)$ into individual band contribution $\chi_{\text{inter},\alpha}(\mu)$ is quite meaningless. A natural issue is thus how to decompose $\chi_{\text{inter}}(\mu)$ into several contributions $\chi_\lambda(\mu)$ that are independently meaningful. From that perspective and as explained in the previous sections, in the present work $\chi_{\text{inter}}(\mu)$ is decomposed into three contributions χ_Ω, χ_g, and $\tilde{\chi}_g$, that each verifies the following two properties: (i) it vanishes outside the full band spectrum, (ii) it verifies the tight-binding sum rule $\int d\mu \ \chi_{\Omega,g,\tilde{g}}(\mu) = 0$, despite the fact that they all contain a Fermi sea part.

In the following, the discussion focuses on two works that provide an explicit decomposition of the interband susceptibility χ_{inter} into several distinct contributions. The first one is Blount's pioneer work [7] in which some interband contributions explicitly imply the orbital magnetic moment and the Berry curvature (note that the Berry curvature concept and terminology did not exist at that time). The second one is the recent semiclassical wave packet approach developed in Refs. [16,29], where it was shown that some interband contributions explicitly imply the quantum metric.

A. Blount's decomposition of χ_{inter}

More than fifty years ago, Blount [7] proposed a decomposition of χ_{inter} into six distinct contributions. More precisely by defining $\chi_{\text{inter}}(\mu) = -\frac{\partial^2}{\partial \mathbf{B}^2} F_{\text{inter}}(\mu, \mathbf{B})$, Blount writes the grand potential $F = F_{\text{LP}} + F_{\text{inter}}$ with

$$F_{\text{inter}} = F_{\text{Pauli}} + F_\Omega + F_{\text{VV}} + F_{\text{at}} + F_{\text{pa}} + F_7, \qquad (35)$$

and where each contribution is given by

$$F_{\text{Pauli}} = \left\langle n'_\alpha \frac{1}{2}(\boldsymbol{B} \cdot \boldsymbol{\mathcal{M}}_\alpha)^2 \right\rangle_{\text{BZ}},$$

$$F_\Omega = \left\langle -n_\alpha \frac{3}{4}(\boldsymbol{B} \cdot \boldsymbol{\mathcal{M}}_\alpha)(\boldsymbol{B} \cdot \boldsymbol{\Omega}_\alpha) \right\rangle_{\text{BZ}},$$

$$F_{\text{VV}} = \left\langle n_\alpha \sum_{\beta \neq \alpha} \frac{|\sum_{\beta' \neq \alpha} \boldsymbol{\mathscr{A}}_{\alpha\beta'} \cdot (\boldsymbol{V}_{\beta'\beta} + \boldsymbol{v}_\alpha \delta_{\beta\beta'})|^2}{\varepsilon_\alpha - \varepsilon_\beta} \right\rangle_{\text{BZ}},$$

$$F_{\text{at}} = \left\langle n_\alpha \frac{1}{2} \sum_{\beta \neq \alpha} \frac{\boldsymbol{\mathscr{A}}_{\alpha\beta} \cdot \boldsymbol{\mathscr{A}}_{\beta\alpha}}{m} \right\rangle_{\text{BZ}},$$

$$F_{\text{pa}} = \left\langle -n_\alpha \frac{1}{2} \sum_{\beta \neq \alpha} (\mathscr{A}_i)_{\alpha\beta}(\mathscr{A}_j)_{\beta\alpha} \partial^2_{ij} \varepsilon_\alpha \right\rangle_{\text{BZ}},$$

$$F_7 = \left\langle n'_\alpha \frac{1}{2} \boldsymbol{v}_\alpha \cdot \left[\sum_{\beta,\beta' \neq \alpha} (\boldsymbol{\mathscr{A}}_{\alpha\beta}(\boldsymbol{V}_{\beta'\beta} + \boldsymbol{v}_\alpha \delta_{\beta\beta'}) \cdot \boldsymbol{\mathscr{A}}_{\beta'\alpha} + \text{c.c}) \right] \right\rangle_{\text{BZ}}, \qquad (36)$$

with the notations

$$\boldsymbol{V}_{\alpha\beta} = \langle u_\alpha | \nabla_{\boldsymbol{k}} \hat{h} | u_\beta \rangle,$$

$$\boldsymbol{v}_\alpha = \boldsymbol{V}_{\alpha\alpha} = \nabla_{\boldsymbol{k}} \varepsilon_\alpha,$$

$$\boldsymbol{A}_{\alpha\beta} = \langle u_\alpha | i \nabla_{\boldsymbol{k}} | u_\beta \rangle = -i \frac{\boldsymbol{V}_{\alpha\beta}}{\varepsilon_\alpha - \varepsilon_\beta},$$

$$\boldsymbol{\mathcal{M}}_\alpha = \frac{1}{2} \sum_{\beta \neq \alpha} \boldsymbol{A}_{\alpha\beta} \times \boldsymbol{V}_{\beta\alpha}.$$

$$\boldsymbol{\Omega}_\alpha = i \sum_{\beta \neq \alpha} \boldsymbol{A}_{\alpha\beta} \times \boldsymbol{A}_{\beta\alpha},$$

$$\boldsymbol{\mathscr{A}}_{\alpha\beta} = \frac{1}{2} \boldsymbol{B} \times \boldsymbol{A}_{\alpha\beta}. \qquad (37)$$

All these expressions were derived starting from the Schrödinger Hamiltonian $\hat{H} = \frac{p^2}{2m} + V(\boldsymbol{r})$ in a periodic lattice potential $V(\boldsymbol{r})$ such that m is the bare electron mass. The effect of the crystal lattice is implicitly taken into account through the existence of an infinite number of bands with effective dispersions $\varepsilon_\alpha(\boldsymbol{k})$ and associated cell-periodic Bloch states $|u_\alpha\rangle$.

In Eqs. (36), the contribution F_{Pauli} is Fermi surface like and represents the effective Pauli paramagnetism of the orbital magnetic moment $\boldsymbol{\mathcal{M}}_\alpha$ of the αth band. The contribution F_Ω involves the product of the orbital magnetic moment by a quantity $\boldsymbol{\Omega}_\alpha$ which appears to be the Berry curvature. F_Ω is Fermi sea like, and Blount argued that it is diamagnetic. The third contribution represents the Van-Vleck paramagnetism of occupied bands; it involves interband geometric effect through the interband Berry connection $\boldsymbol{A}_{\alpha\beta}$ or interband velocity operator $\boldsymbol{V}_{\alpha\beta}$. The fourth and fifth terms are argued to constitute generalization of the Langevin atomic diamagnetism for electrons in occupied bands. In particular the fourth term is clearly diamagnetic whereas the sign of the fifth may change according to the band dispersion. The last term F_7 is Fermi surface like, but its meaning remains unclear.

Due to the very different starting point, it may appear quite difficult to compare Blount's results with the tight-binding approach, involving a finite number of band, considered in this work. Nevertheless it appears instructive to arbitrarily substitute the peculiar form of the Berry connection properties of two-band models into Blount's formula (for a magnetic field $\boldsymbol{B}$ perpendicular to a 2D plane). In doing this, each Blount's susceptibility contribution rewrites:

$$\chi_{\text{Pauli}} = \langle -n'_\alpha \varepsilon^2 \Omega^2 \rangle_{\text{BZ}},$$

$$\chi_\Omega = \left\langle n_\alpha \frac{3}{2} \alpha \varepsilon \Omega^2 \right\rangle_{\text{BZ}},$$

$$\chi_{\text{VV}} = \langle -n_\alpha g^{ij} \partial_i \varepsilon_0 \partial_j \varepsilon_0 \rangle_{\text{BZ}},$$

$$\chi_{\text{at}} = \left\langle n_\alpha \frac{1}{4m} g^{ij} \delta_{ij} \right\rangle_{\text{BZ}},$$

$$\chi_{\text{pa}} = \left\langle -n_\alpha \frac{1}{4} g^{ij} \partial^2_{ij} \varepsilon_\alpha \right\rangle_{\text{BZ}},$$

$$\chi_7 = \langle n'_\alpha g^{ij} \partial_i \varepsilon_\alpha \partial_j \varepsilon_0 \rangle_{\text{BZ}} = \langle -n_\alpha \partial_i (g^{ij} \partial_j \varepsilon_0) \rangle_{\text{BZ}}, \qquad (38)$$

where an integration by part permits us to rewrite χ_7 also as a Fermi sea term.

By summing the two Blount contributions that depend on the Berry curvature it appears that $\chi_{\text{Pauli}} + \chi_\Omega$ is similar but differs by a numerical factor from the corresponding tight-binding contribution χ_Ω (19). More precisely Blount's Fermi sea term χ_Ω is a factor 3/2 bigger than in Eq. (19); as a result $\chi_{\text{Pauli}} + \chi_\Omega$ cannot verify the sum rule. By contrast, it appears that Blount's contributions χ_{VV} and χ_7 correspond perfectly to the first and second part of the contribution $\tilde{\chi}_g$ in Eqs. (20) and (22); as a result $\chi_{\text{VV}} + \chi_7$ verifies the sum rule. The last

two terms χ_{at} and χ_{pa} are, however, very different from the last contribution χ_g obtained for two-band tight-binding models.

From the above analysis one may conclude that the three contributions χ_Ω, χ_{at}, and χ_{pa} of Blount need to be modified in order to recover the two-band tight-binding formula. In fact, it appears that only χ_{at} needs to be revised (see below) [16]. To conclude with Blount's formula, we note that for centrosymmetric systems ($\chi_{\text{Pauli}} = \chi_\Omega = 0$), contributions identical to $\chi_{\text{VV}}, \chi_{\text{at}}, \chi_{\text{pa}}$, and χ_7 were recently derived [40] starting from the Fukuyama [10,11] compact Green's function formula.

B. Gao *et al.* decomposition of χ_{inter}

Using a semiclassical wave packets method, Gao *et al.* [16] recently presented a decomposition of the interband contribution $F_{\text{inter}}(\mu)$ into five terms:

$$F_{\text{inter}} = F_{\text{Pauli}} + F_{\text{geom}} + F_{\text{Polar}} + F_{\text{VV}} + F_{\text{Langevin}}, \quad (39)$$

which are given by

$$F_{\text{Pauli}} = \left\langle -n_\alpha' \frac{1}{2}(\boldsymbol{B} \cdot \boldsymbol{\mathcal{M}}_\alpha)^2 \right\rangle_{\text{BZ}},$$

$$F_{\text{geom}} = \left\langle n_\alpha \left[\left(\frac{3}{4}(\boldsymbol{B} \cdot \boldsymbol{\mathcal{M}}_\alpha)(\boldsymbol{B} \cdot \boldsymbol{\Omega}_\alpha) \right. \right. \right.$$
$$\left. \left. \left. + \frac{1}{8}\epsilon_{sik}\epsilon_{tjl} B_s B_t g_{\alpha ij} \partial_{kl}^2 \varepsilon_\alpha \right) \right] \right\rangle_{\text{BZ}},$$

$$F_{\text{Polar}} = \left\langle n_\alpha' \frac{1}{4} \boldsymbol{v}_\alpha \cdot \boldsymbol{P}_\alpha \right\rangle_{\text{BZ}},$$

$$F_{\text{VV}} = \left\langle -n_\alpha \sum_{\beta \neq \alpha} \frac{\boldsymbol{G}_{\alpha\beta}\boldsymbol{G}_{\beta\alpha}}{\varepsilon_\alpha - \varepsilon_\beta} \right\rangle_{\text{BZ}},$$

$$F_{\text{Langevin}} = \left\langle -n_\alpha \frac{1}{8} \left[\sum_{\beta,\beta' \neq \alpha} (\boldsymbol{B} \times \boldsymbol{A}_{\alpha\beta})_i (\Gamma_{ij})_{\beta\beta'} (\boldsymbol{B} \times \boldsymbol{A}_{\alpha\beta})_j \right. \right.$$
$$\left. \left. - \frac{1}{2}(\boldsymbol{B} \times \nabla)_i (\boldsymbol{B} \times \nabla)_j (\Gamma_{ij})_{\alpha\alpha} \right] \right\rangle_{\text{BZ}}, \quad (40)$$

where ϵ_{ijk} is the totally antisymmetric tensor and with

$$g_{\alpha ij} = \frac{1}{2} \sum_{\beta \neq \alpha} \left[(\boldsymbol{A}_{\alpha\beta})_i (\boldsymbol{A}_{\beta\alpha})_j + \text{c.c} \right],$$

$$\boldsymbol{P}_\alpha = \frac{1}{4} \sum_{\beta,\beta' \neq \alpha} [(\boldsymbol{B} \times \boldsymbol{A}_{\alpha\beta})(\boldsymbol{v}_\alpha \delta_{\beta\beta'}$$
$$+ \boldsymbol{V}_{\beta\beta'}) \cdot (\boldsymbol{B} \times \boldsymbol{A}_{\beta'\alpha}) + \text{c.c}],$$

$$\boldsymbol{G}_{\alpha\beta} = -\frac{1}{2}\boldsymbol{B} \cdot \left[\sum_{\beta' \neq \beta} (\boldsymbol{V}_{\alpha\beta'} + \boldsymbol{v}_\beta \delta_{\alpha\beta'}) \times \boldsymbol{A}_{\beta'\beta} \right],$$

$$(\Gamma_{ij})_{\alpha\beta} = \langle u_\alpha | \partial_{ij}^2 \hat{h} | u_\beta \rangle, \quad (41)$$

where the quantities $g_{\alpha ij}$ and $\boldsymbol{P}_\alpha$ correspond, respectively, to the quantum metric tensor and the polarization associated to the αth band, where in fact the polarization is argued to constitute another characteristic geometric quantity [16].

Despite the very different derivation and some change of notation, as compared to Blount, it is apparent that there

are strong similarities between Blount's formula Eqs. (36) and Gao *et al.*'s expressions Eqs. (40). More precisely, it is easily shown that $F_{\text{Pauli}}, F_{\text{VV}}$ are identical and moreover $F_{\text{geom}} = F_\Omega + F_{\text{pa}}$ and $F_{\text{Polar}} = \frac{1}{2}F_7$. Apart from the *wrong* factor $1/2$ of F_{Polar} (which has been already pointed out in Ref. [40]), the main apparent difference between Blount and Gao *et al.* formulations resides in the contribution F_{at} for the former which becomes F_{Langevin} in the latter. In fact when considering the same starting Hamiltonian [e.g., $\hat{H} = \frac{p^2}{2m} + V(\boldsymbol{r})$ in a periodic lattice potential $V(\boldsymbol{r})$] it appears that $(\Gamma_{ij})_{\alpha\beta} = \frac{1}{m}\delta_{ij}\delta_{\alpha\beta}$, with m the bare electron mass, such that in this situation $F_{\text{Langevin}} = F_{\text{at}}$.

More interestingly, when considering generic two-bands tight-binding models, as in the present work, it is possible to show that in such a situation the Langevin term gives rise to a susceptibility contribution of the form:

$$\chi_{\text{Langevin}} = \left\langle -n_\alpha \left[\frac{1}{4} g^{ij} \partial_{ij}^2 \varepsilon_\alpha + \frac{1}{2}\alpha\varepsilon\Omega^2 + \frac{1}{2}\alpha \frac{\partial_i(\varepsilon^2 \partial_j g^{ij})}{\varepsilon} \right] \right\rangle_{\text{BZ}}. \quad (42)$$

Using this expression it is immediate to establish the following identities (valid for two-band models)

$$\chi_\Omega + \chi_g = \chi_{\text{Pauli}} + \chi_{\text{geom}} + \chi_{\text{Langevin}},$$
$$\tilde{\chi}_g = \chi_{\text{VV}} + 2\chi_{\text{Polar}}, \quad (43)$$

where in the first line there is a complete cancellation of the term $\langle n_\alpha \frac{1}{4} g^{ij} \partial_{ij}^2 \varepsilon_\alpha \rangle_{\text{BZ}}$ present in both χ_{geom} and χ_{Langevin} but with opposite sign. This cancellation is important because it can be checked that this term generically gives rise to an unphysical finite susceptibility plateau that extends to $\mu \to \infty$ when each contribution χ_{geom} and χ_{Langevin} are considered separately. An indication of this spurious plateau for each contribution is already visible in Fig. 2(b) of Gao *et al.* [16], despite the reduced range of μ.

VII. CONCLUSION AND PERSPECTIVES

This study shows the physical richness of the orbital susceptibility even in the simplest case of two coupled bands. We have stressed that the Berry curvature Ω is not sufficient to describe interband effects which are still prominent even when $\Omega = 0$, as shown for the square lattice with staggered potential (broken sublattice symmetry). A simple model in which inversion symmetry is progressively broken shows how the complexity of the orbital response is driven by the structure of a quantum geometric tensor, whose antisymmetric part is the Berry curvature and the symmetric part (*the quantum metric*) carries information on the distance between Bloch states in Hilbert space. The complex structure of the susceptibility can be summarized by its value in the gap which shows explicitly the contributions related to the Berry curvature Ω and the metric tensor g_{ij}:

$$\chi_{\text{gap}} = \left\langle \frac{1}{\varepsilon}\left(-\varepsilon^2 \Omega^2 + \frac{1}{2}\partial_i(\varepsilon^2 \partial_j g^{ij}) + g^{ij}\partial_i \varepsilon_0 \partial_j \varepsilon_0 \right) \right\rangle_{\text{BZ}}.$$

The surprising strong influence of a flat band even in the simplest case of a two-band model motivates further the study of flat band physics in multiband systems. On a more

general perspective, the orbital susceptibility may be an important tool for the investigation of topological transitions in multiband systems since it provides unique information on the evolution of the geometric properties of Bloch states across such transitions.

ACKNOWLEDGMENTS

APPENDIX A: ORBITAL SUSCEPTIBILITY OF TWO-BAND MODELS

1. Explicit derivation

This section presents the main calculation steps of the four contributions χ_{LP}, χ_Ω, χ_g, and $\tilde{\chi}_g$. To start with, the general susceptibility formula Eq. (1) (main text) is rewritten in the form

$$\chi_{orb}(\mu, T) = -\frac{\mu_0 e^2}{12\hbar^2} \frac{\Im m}{\pi S} \int_{-\infty}^{\infty} dE\, n_F(E)$$
$$\times \int_{BZ} \frac{d^2k}{4\pi^2} (U(\boldsymbol{k}, E) + V(\boldsymbol{k}, E)) \quad (A1)$$

with

$$U(\boldsymbol{k}, E) = \text{tr}\{(\hat{g}\partial_{xx}\hat{h}\hat{g}\partial_{yy}\hat{h} - \hat{g}\partial_{xy}\hat{h}\hat{g}\partial_{xy}\hat{h})_{\boldsymbol{k}}\},$$
$$V(\boldsymbol{k}, E) = 2\,\text{tr}\{([\hat{g}\partial_x\hat{h}, \hat{g}\partial_y\hat{h}]^2)_{\boldsymbol{k}}\} \quad (A2)$$

where $\text{tr}\{\bullet\}$ is the partial trace operator on the band index $\alpha = \pm$. By using similar steps as described in Appendix D of Ref. [25], one obtains

$$U = \sum_\alpha g_\alpha^2 U_\alpha^{(1)} + g_\alpha g_{-\alpha} U^{(2)},$$
$$V = \sum_\alpha g_\alpha^3 g_{-\alpha} V_\alpha^{(1)} + g_\alpha^2 g_{-\alpha}^2 V^{(2)} \quad (A3)$$

with $g_\alpha(\boldsymbol{k}, E) = \frac{1}{E - \varepsilon_\alpha(\boldsymbol{k})}$ and where

$$U_\alpha^{(1)}(\boldsymbol{k}) = (\partial_{xx}\varepsilon_\alpha \partial_{yy}\varepsilon_\alpha - \partial_{xy}\varepsilon_\alpha \partial_{xy}\varepsilon_\alpha)$$
$$+ 4(\varepsilon^2 \Omega^2 - \alpha\varepsilon g^{ij}\partial_{ij}\varepsilon_\alpha),$$
$$U^{(2)}(\boldsymbol{k}) = -4(\varepsilon^2\Omega^2 + \tfrac{1}{2}\partial_{ij}(\varepsilon^2 g^{ij}) - \varepsilon g^{ij}\partial_{ij}\varepsilon),$$
$$V_\alpha^{(1)}(\boldsymbol{k}) = -16\epsilon^2 g^{ij}\partial_i\varepsilon_\alpha \partial_j\varepsilon_\alpha,$$
$$V^{(2)}(\boldsymbol{k}) = -16\varepsilon^2(2\varepsilon^2\Omega^2 - g^{ij}\partial_i\varepsilon_\alpha \partial_j\varepsilon_{-\alpha}). \quad (A4)$$

At this point, using the identity $\partial_i(g_\alpha^n) = n g_\alpha^{n+1}\partial_i\varepsilon_\alpha$ and integration by part, the following identity is established:

$$\int_{BZ} \frac{d^2k}{4\pi^2} \sum_\alpha g_\alpha^3 g_{-\alpha} V_\alpha^{(1)}$$
$$= \int_{BZ} \frac{d^2k}{4\pi^2} \sum_\alpha 8\left[g_\alpha^2 g_{-\alpha}^2 (\epsilon^2 g^{ij}\partial_i\varepsilon_\alpha \partial_j\varepsilon_{-\alpha}) \right.$$
$$\left. + g_\alpha^2 g_{-\alpha}(\epsilon^2 g^{ij}\partial_{ij}\varepsilon_\alpha) - \frac{1}{2} g_\alpha g_{-\alpha}\partial_{ij}(\varepsilon^2 g^{ij}) \right]. \quad (A5)$$

From there, by using the equalities

$$g_\alpha g_{-\alpha} = \frac{\alpha}{2\varepsilon}(g_\alpha - g_{-\alpha}),$$
$$g_\alpha^2 g_{-\alpha}^2 = \frac{1}{4\varepsilon^2}(g_\alpha^2 + g_{-\alpha}^2 - 2g_\alpha g_{-\alpha}),$$
$$g_\alpha^2 g_{-\alpha} = \frac{\alpha}{2\varepsilon}(g_\alpha^2 - g_\alpha g_{-\alpha}), \quad (A6)$$

it is possible to rewrite Eq. (A3) as

$$U = \sum_\alpha g_\alpha^2 U_\alpha^{(1)} + \alpha\frac{g_\alpha}{\varepsilon}U^{(2)},$$
$$V = \sum_\alpha g_\alpha^2 \tilde{V}_\alpha^{(1)} + \alpha\frac{g_\alpha}{\varepsilon}\tilde{V}^{(2)} \quad (A7)$$

with

$$\tilde{V}_\alpha^{(1)}(\boldsymbol{k}) = 4(-4\varepsilon^2\Omega^2 + 3g^{ij}\partial_i\varepsilon_\alpha \partial_j\varepsilon_{-\alpha} + \alpha\varepsilon g^{ij}\partial_{ij}\varepsilon_\alpha),$$
$$\tilde{V}^{(2)}(\boldsymbol{k}) = -4(-4\varepsilon^2\Omega^2 + 3g^{ij}\partial_i\varepsilon_\alpha \partial_j\varepsilon_{-\alpha} + \varepsilon g^{ij}\partial_{ij}\varepsilon$$
$$+ \partial_{ij}(\epsilon^2 g^{ij})). \quad (A8)$$

Summing U and V yields

$$\frac{U + V}{12} = \sum_\alpha g_\alpha^2 \left[\frac{1}{12}(\partial_{xx}\varepsilon_\alpha\partial_{yy}\varepsilon_\alpha - \partial_{xy}\varepsilon_\alpha\partial_{xy}\varepsilon_\alpha) - \varepsilon^2\Omega^2 \right.$$
$$\left. + g^{ij}\partial_i\varepsilon_\alpha\partial_j\varepsilon_{-\alpha} \right]$$
$$+ \alpha\frac{g_\alpha}{\varepsilon}\left[\varepsilon^2\Omega^2 - g^{ij}\partial_i\varepsilon_\alpha\partial_j\varepsilon_{-\alpha} - \frac{1}{2}\partial_{ij}(\varepsilon^2 g^{ij}) \right]. \quad (A9)$$

The final step consists of performing the explicit integral over variable E by using the identity

$$\Im m \int_{-\infty}^{+\infty} \frac{n_F(E)}{(E - \varepsilon_\alpha)^k} dE = -\frac{\pi}{k!} n_F^{(k)}(\varepsilon_\alpha), \quad (A10)$$

where $n_F^{(k)}$ is the kth derivative of the Fermi function $n_F(\varepsilon) = 1/[e^{\beta(\varepsilon - \mu)} + 1]$. In order to shorten the expressions, the susceptibility is written in units of $\frac{\mu_0 e^2}{\hbar^2}$ and the main text shorthand notations are introduced

$$n_\alpha \equiv n_F(\varepsilon_\alpha(\boldsymbol{k})), \quad \langle\cdots\rangle_{BZ} \equiv \sum_{\alpha=\pm}\int\cdots\frac{d^2k}{4\pi^2}. \quad (A11)$$

The different terms appearing in Eq. (A9) then give rise to the different susceptibility contributions:

$$\chi_{orb} = \chi_{LP} + \chi_\Omega + \chi_g + \tilde{\chi}_g, \quad (A12)$$

with

$$\chi_{LP} = \left\langle \frac{n_\alpha'}{12}(\partial_{xx}\varepsilon_\alpha\partial_{yy}\varepsilon_\alpha - \partial_{xy}\varepsilon_\alpha\partial_{xy}\varepsilon_\alpha) \right\rangle_{BZ}, \quad (A13)$$
$$\chi_\Omega = \left\langle \left(-n_\alpha' + \alpha\frac{n_\alpha}{\varepsilon}\right)\mathscr{M}^2 \right\rangle_{BZ}, \quad \mathscr{M} = \varepsilon\Omega \quad (A14)$$

and

$$\chi_g + \tilde{\chi}_g$$
$$= \left\langle \left(n'_\alpha - \alpha \frac{n_\alpha}{\varepsilon} \right) g^{ij} \partial_i \varepsilon_\alpha \partial_j \varepsilon_{-\alpha} - \alpha \frac{n_\alpha}{\varepsilon} \frac{1}{2} \partial_{ij} (\varepsilon^2 g^{ij}) \right\rangle_{\text{BZ}}.$$
(A15)

There are different ways to write the separate contributions χ_g and $\tilde{\chi}_g$. The following compact expressions are obtained by performing integrations by part in order to eliminate all Fermi surface contributions:

$$\chi_g = \left\langle -\alpha \frac{n_\alpha}{\varepsilon} Z_g \right\rangle_{\text{BZ}}, \qquad \tilde{\chi}_g = \left\langle -\alpha \frac{n_\alpha}{\varepsilon} \tilde{Z}_g \right\rangle_{\text{BZ}} \quad (A16)$$

with

$$Z_g = \frac{1}{2} \partial_j (\varepsilon^2 \partial_i g^{ij}), \quad \tilde{Z}_g = g^{ij} \partial_i \varepsilon_0 \partial_j \varepsilon_0 + \alpha \varepsilon \partial_i (\partial_j \varepsilon_0 g^{ij}).$$
(A17)

To conclude, it is worth mentioning that the distinct susceptibility contributions verify separately the sum rule over the full zero-field spectrum:

$$\int d\mu \chi_{\text{LP}}(\mu) = \int d\mu \chi_\Omega(\mu) = \int d\mu \chi_g(\mu)$$
$$= \int d\mu \tilde{\chi}_g(\mu) = 0. \quad (A18)$$

Furthermore each susceptibility contribution vanishes for μ outside the full spectrum. These last two properties, together with the rather natural interpretation of each contribution (see below) strengthens the above decomposition of χ_{inter} into three terms in comparison with the various decompositions adopted in other works (see below) [7,16,40].

2. Role of symmetries on interband susceptibility contributions $\chi_\Omega, \chi_g, \tilde{\chi}_g$

As already mentioned in the main text, for systems that are time-reversal invariant, inversion and particle-hole symmetries permit us to discriminate the three interband susceptibility contributions $\chi_\Omega, \chi_g, \tilde{\chi}_g$. For systems with an inversion symmetry, the Berry curvature vanishes [$\Omega(\mathbf{k}) = 0$] and therefore $\chi_\Omega(\mu) = 0$ (from that perspective, the case of graphene should be understood as the zero gap limit of a system that breaks inversion symmetry such as boron nitride). Similarly, systems with particle-hole symmetry [$\varepsilon_0(\mathbf{k}) = 0$] verify $\tilde{\chi}_g(\mu) = 0$. The contribution $\chi_g(\mu)$ is thus the only one that remains when both inversion and particle-hole symmetries are simultaneously present. In that respect it may be seen as the most fundamental one.

Beyond global symmetries, it nevertheless appears that χ_g vanishes for systems such that $\mathbf{h}(\mathbf{k})$ only depends on

either k_x or k_y. For such a case, the metric tensor has a single nonvanishing component g_{xx} or g_{yy}, and therefore χ_g and χ_Ω both vanish. In that situation the only nonvanishing component is $\tilde{\chi}_g$. A simple example is a square lattice with nearest neighbor hopping t and an alternating onsite potential $\pm\Delta$ along the x direction. The corresponding Hamiltonian matrix is constructed from $\varepsilon_0 = 2t \cos(k_y)$ and $\mathbf{h}(\mathbf{k}) = (2t \cos(k_x), 0, \Delta)$.

APPENDIX B: FIELD INDUCED POSITIONAL SHIFT IN TWO-BAND SYSTEMS

Very recently it was shown that the presence of a magnetic field induces a band dependent positional shift of the Berry connection such that $\mathbf{a}_\alpha \to \mathbf{a}_\alpha + B\mathbf{a}'_\alpha$, to linear order in magnetic field [16,29]. (Here $a'(\mathbf{k})$ does not contain the magnetic field, so that the full Berry connection is $a(\mathbf{k}) + a'(\mathbf{k})B$.) According to the semiclassical wave packet formalism [16,29], the positional shift is composed of two distinct contributions so that $\mathbf{a}'_\alpha(\mathbf{k})$ can be written

$$\mathbf{a}'_\alpha = \mathbf{a}_g + \alpha \tilde{\mathbf{a}}_g, \quad (B1)$$

where the contribution $\mathbf{a}_g$ originates from the horizontal mixing of zero field band eigenstates whereas the contribution $\tilde{\mathbf{a}}_g$ comes from further vertical mixing of band eigenstates [16,29]. For two-band systems in two dimensions and in a perpendicular magnetic field, the positional shift contributions $\mathbf{a}_g$ and $\tilde{\mathbf{a}}_g$ take the form

$$\mathbf{a}_g(\mathbf{k}) = \frac{\mathbf{B}}{B} \times \frac{1}{2} \begin{pmatrix} \partial_j g^{xj} \\ \partial_j g^{yj} \\ 0 \end{pmatrix}, \quad \tilde{\mathbf{a}}_g(\mathbf{k}) = \frac{\mathbf{B}}{B} \times \frac{1}{\varepsilon} \begin{pmatrix} g^{xj} \partial_j \varepsilon_0 \\ g^{yj} \partial_j \varepsilon_0 \\ 0 \end{pmatrix}.$$
(B2)

Defining the corresponding field induced shifts of the Berry curvature,

$$\Omega_g(\mathbf{k}) = [\nabla_{\mathbf{k}} \times \mathbf{a}_g]_z = -\frac{1}{2} \partial_i \partial_j g^{ij} \quad (B3)$$

and

$$\tilde{\Omega}_g(\mathbf{k}) = [\nabla_{\mathbf{k}} \times \tilde{\mathbf{a}}_g]_z = -\partial_i \left(\frac{g^{ij} \partial_j \varepsilon_0}{\varepsilon} \right), \quad (B4)$$

it is clear that each of them is an even function in $\mathbf{k}$-space $\Omega_g(\mathbf{k}) = \Omega_g(-\mathbf{k})$ and similarly for $\tilde{\Omega}_g(\mathbf{k})$, which is to be expected since it depends on the magnetic field that explicitly breaks time-reversal symmetry. Despite this, each Berry curvature shift verifies the sum rule $\int_{\text{BZ}} d^2k \, \Omega_g(\mathbf{k}) = \int_{\text{BZ}} d^2k \, \tilde{\Omega}_g(\mathbf{k}) = 0$.

---

[1] N. W. Ashcroft and N. D. Mermin, *Solid State Physics* (Saunders College Publishing, Fort Worth, 1976).

[2] L. D. Landau, Z. Phys. **64**, 629 (1930); see also the *Collected papers of L. D. Landau* edited by D. ter Haar (Pergamon Press, New York, 1965).

[3] R. Peierls, Z. Phys. **80**, 763 (1933).

[4] E. N. Adams, Phys. Rev. **89**, 633 (1953).

[5] J. E. Hebborn and E. H. Sondheimer, J. Phys. Chem. Solids **13**, 105 (1960).

[6] L. M. Roth, J. Phys. Chem. Solids **23**, 433 (1962).

[7] E. I. Blount, Phys. Rev. **126**, 1636 (1962).

[8] G. H. Wannier, Phys. Rev. **136**, A803 (1964).

[9] P. K. Misra and L. M. Roth, Phys. Rev. **177**, 1089 (1969).

[10] H. Fukuyama, Prog. Theor. Phys. **45**, 704 (1971).

[11] H. Fukuyama, J. Phys. Soc. Jpn. **28**, 570 (1970).

[12] D. Xiao, M. C. Chang, and Q. Niu, Rev. Mod. Phys. **82**, 1959 (2010).

[13] T. Thonhauser, Int. J. Mod. Phys B **25**, 1429 (2011).

[14] T. Thonhauser, D. Ceresoli, D. Vanderbilt, and R. Resta, Phys. Rev. Lett. **95**, 137205 (2005).

[15] D. Xiao, J. Shi, and Q. Niu, Phys. Rev. Lett. **95**, 137204 (2005).

[16] Y. Gao, S. A. Yang, and Q. Niu, Phys. Rev. B **91**, 214405 (2015).

[17] M. V. Berry, *The quantum phase, five years after* in *Geometric Phases in Physics*, edited by A. Shapere and F. Wilczek (World Scientific, Singapore, 1989).

[18] J. P. Provost and G. Vallee, Commun. Math. Phys. **76**, 289 (1980).

[19] N. Marzari and D. Vanderbilt, Phys. Rev. B **56**, 12847 (1997).

[20] R. Resta, Eur. Phys. J. B **79**, 121 (2011).

[21] T. Neupert, C. Chamon, and C. Mudry, Phys. Rev. B **87**, 245103 (2013).

[22] S. Peotta and P. Törmä, Nat. Commun. **6**, 8944 (2015).

[23] A. Srivastava and A. Imamoğlu, Phys. Rev. Lett. **115**, 166802 (2015).

[24] L.-K. Lim, J.-N. Fuchs, and G. Montambaux, Phys. Rev. A **92**, 063627 (2015).

[25] A. Raoux, F. Piéchon, J.-N. Fuchs, and G. Montambaux, Phys. Rev. B **91**, 085120 (2015).

[26] G. Gomez-Santos and T. Stauber, Phys. Rev. Lett. **106**, 045504 (2011).

[27] A. Raoux, M. Morigi, J. N. Fuchs, F. Piéchon, and G. Montambaux, Phys. Rev. Lett. **112**, 026402 (2014).

[28] A. Gutiérrez-Rubio, T. Stauber, G. Gòmez-Santos, R. Asgari, and F. Guinea, Phys. Rev. B **93**, 085133 (2016).

[29] Y. Gao, S. A. Yang, and Q. Niu, Phys. Rev. Lett. **112**, 166601 (2014); here $a'(\boldsymbol{k})$ does not contain the magnetic field, so that the full Berry connection is $a(\boldsymbol{k}) + a'(\boldsymbol{k})B$.

[30] G. Vignale, Phys. Rev. Lett. **67**, 358 (1991).

[31] M. Koshino and T. Ando, Phys. Rev. B **81**, 195431 (2010).

[32] L. Tarruell, D. Greif, T. Uehlinger, G. Jotzu, and T. Esslinger, Nature (London) **483**, 302 (2012).

[33] L.-K. Lim, J.-N. Fuchs, and G. Montambaux, Phys. Rev. Lett. **108**, 175303 (2012).

[34] J. W. McClure, Phys. Rev. **104**, 666 (1956).

[35] J. N. Fuchs, F. Piéchon, M. O. Goerbig, and G. Montambaux, Eur. Phys. J. B **77**, 351 (2010).

[36] A. Mielke, J. Phys. A **24**, 3311 (1991).

[37] H. Aoki, M. Ando, and H. Matsumura, Phys. Rev. B **54**, R17296(R) (1996).

[38] H. Tasaki, Phys. Rev. Lett. **69**, 1608 (1992).

[39] B. Savoie, J. Math. Phys. **53**, 073302 (2012).

[40] M. Ogata and H. Fukuyama, J. Phys. Soc. Jpn. **84**, 124708 (2015).